We are IntechOpen, the world's leading publisher of Open Access books Built by scientists, for scientists

4,800
Open access books available

122,000
International authors and editors

135M
Downloads

Our authors are among the

154
Countries delivered to

TOP 1%
most cited scientists

12.2%
Contributors from top 500 universities

CLARIVATE ANALYTICS BOOK CITATION INDEX INDEXED

WEB OF SCIENCE™

Selection of our books indexed in the Book Citation Index in Web of Science™ Core Collection (BKCI)

Interested in publishing with us?
Contact book.department@intechopen.com

Numbers displayed above are based on latest data collected.
For more information visit www.intechopen.com

5

Ferroelectric Materials for Small-Scale Energy Harvesting Devices and Green Energy Products

Mickaël Lallart and Daniel Guyomar
LGEF, INSA-Lyon
France

1. Introduction

Portable electronic devices and autonomous systems experienced a strong development over the last few years, thanks to progresses in microelectronics and ultralow-power circuits, as well as because of an increasing demand in autonomous and "left-behind" sensors from various industrial fields (for instance aeronautic, civil engineering, biomedical engineering, home automation). Until now, such devices have been powered using primary batteries. However, such a solution is often inadequate as batteries raise maintenance issues because of their limited lifespan (typically one year under normal conditions - Roundy, Wright and Rabaey (2003)) and complex recycling process (leading to environmental problems). In order to tackle these drawbacks, many efforts have been placed over the last decade on systems able to harvest electrical energy from their close environment (Krikke, 2005; Paradiso and Starner, 2005). Many sources are available for power scavenging, such as solar, magnetic, mechanical (vibrations) or thermal (Hudak and Amatucci, 2008). In order to power up small-scale devices, a particular attention has been placed on the last two sources (Anton and Sodano, 2007; Beeby, Tudor and White, 2006; Jia and Liu, 2009; Vullers *et al.*, 2009), as they are commonly available in many environments and because the conversion materials can be easily integrated within the host structure.

The purpose of this chapter is to give a comprehensive view and analysis of small-scale energy harvesting systems using ferroelectric materials, with a special focus on piezoelectric and pyroelectric devices for vibration and thermal energy scavenging systems, respectively. As the energy that can be provided from microgenerators is still limited to the range of tens of microwatts to a few milliwatts, a careful attention has to be placed on the design of the harvester. In particular, backward couplings that may occur between each conversion and energy transfer stages require a global optimization rather than an individual design of each block.

The chapter is organized as follows. Section 2 aims at presenting energy sources and conversion materials that will be considered in this study, as well as basic models for the considered conversion devices. Then section 3 will give a general view of a typical microgenerator, emphasizing the energy conversion chain and issues for optimizing the energy flow. Sections 4 and 5 will focus on two important energy conversion stages (energy conversion and extraction), highlighting general optimization possibilities to get an efficient energy harvester. Implementation issues for realistic applications will then be discussed in

Section 6. Section 7 will present some application examples to self-powered systems. Section 8 will finally briefly conclude the chapter.

2. Energy sources and modeling

Two conversion effects of ferroelectric materials will be considered through this chapter: piezoelectricity, which consists of converting input mechanical energy into electricity, and pyroelectricity, allowing harvesting energy from temperature variations. Therefore, two energy sources will be considered in this study: mechanical energy and thermal energy. The constitutive equations for piezoelectric materials are given by:

$$\begin{cases} \mathrm{d}T = c^E \mathrm{d}S - e^t \mathrm{d}E \\ \mathrm{d}D = \epsilon^S \mathrm{d}E + e\mathrm{d}S \end{cases}, \tag{1}$$

where D, E, S and T respectively refer to electric displacement, electric field, strain and stress tensors. c^E, e and ϵ^S stand for elastic rigidity of the material, piezoelectric coefficient and electric permittivity under constant strain. Finally, d and ^{t} represent the differentiation and transpose operators respectively. In the case of pyroelectric devices, the equations yield:

$$\begin{cases} \mathrm{d}\sigma = p\mathrm{d}E + c\frac{\mathrm{d}\theta}{\theta_0} \\ \mathrm{d}D = \epsilon^\theta \mathrm{d}E + p\mathrm{d}\theta \end{cases}, \tag{2}$$

with θ and θ_0 the temperature and mean temperature, σ the entropy of the system, p the pyroelectric coefficient, c the heat capacitance and ϵ^θ the electric permittivity under constant temperature.

This allows the derivation of energy densities that may be typically obtained. Table 1 gives the comparison of the electrostatic energy density of the two devices for a typical solicitation. It can be seen that the two materials feature relatively close energy density values. This can be explained by the fact that, although piezoelectric coupling is generally much higher than pyroelectric coupling, the input mechanical energy is usually much less than the energy generated by temperature variation. Therefore, the global energy, given by the product of input energy by conversion abilities, is similar for the two materials. Nevertheless, as mechanical frequencies are typically much higher than thermal frequencies, the output power of piezoelectric-based microgenerators is greater than devices using pyroelectric materials (Guyomar *et al.*, 2009; Lallart, 2010a).

Moreover, because of their higher coupling coefficients, extracting energy from piezoelectric elements can affect the mechanical behavior of the system, while the coupling of pyroelectric devices is small enough to neglect the backward coupling (*i.e.*, only the second equation of Eq. (2) can be taken into account).

The model of a global structure can also be obtained from the local constitutive equations Eqs. (1) and (2). In the case of a piezoelectric element (possibly bonded on a structure under

	Piezoelectric	Pyroelectric
Material	NAVY-III type ceramic	PVDF film
Conversion coefficient	$e_{33} = 12.79$ C.m^{-2}	$p = -24e - 6$ C.m^{-2}.K^{-1}
Relative permittivity	$\epsilon_{33}^S/\epsilon_0 = 668$	$\epsilon_{33}^\theta/\epsilon_0 = 12$
Typical input variation	$\Delta S = 10$ μm.m^{-1}	$\Delta\theta = 1$ K
Electrostatic energy density	$(W_{el})_{piezo} = 1.4$ μJ.cm^{-3}	$(W_{el})_{pyro} = 2.7$ μJ.cm^{-3}

Table 1. Energy densities for typical piezoelectric and pyroelectric materials

flexural solicitation), it can be shown that the system may be modeled around one of its resonance frequencies by an electromechanically coupled spring-mass-damper system (Badel *et al.*, 2007; Erturk and Inman, 2008):

$$\begin{cases} M\ddot{u} + C\dot{u} + K_E = F - \alpha V \\ I = \alpha_u \dot{u} - C_0 \dot{V} \end{cases}, \tag{3}$$

where u, F, V and I refer to the displacement (at a particular position of the structure), applied force, piezovoltage and current flowing out of the active material. M, C and K_E denote the dynamic mass, structural damping coefficient and short-circuit stiffness of the system, while α_u and C_0 are given as the force factor and clamped capacitance of the piezoelectric insert.
In the case of pyroelectric energy harvesting, it has previously been stated that the low coupling coefficient permits neglecting the backward coupling. Hence, only the electrical equation is necessary, leading to the macroscopic equation (Guyomar *et al.*, 2009; Lallart, 2010a):

$$I = \alpha_\theta \dot{\theta} - C_0 \dot{V}, \tag{4}$$

with α_θ the pyroelectric factor.

3. Overview of a microgenerator

The principles of an energy harvester lie in several energy conversion and transfer stages to convert the input energy into electrical energy supplied to a load. Basically, four intermediate stages appear between the energy source and the device to power up (Figure 1):

1. Conversion of the raw input energy into effective energy that can be transferred to the active material.
2. Conversion of the energy available in the material into electrical energy.
3. Extraction of the electrical energy available on the material.
4. Storage of the extracted energy.

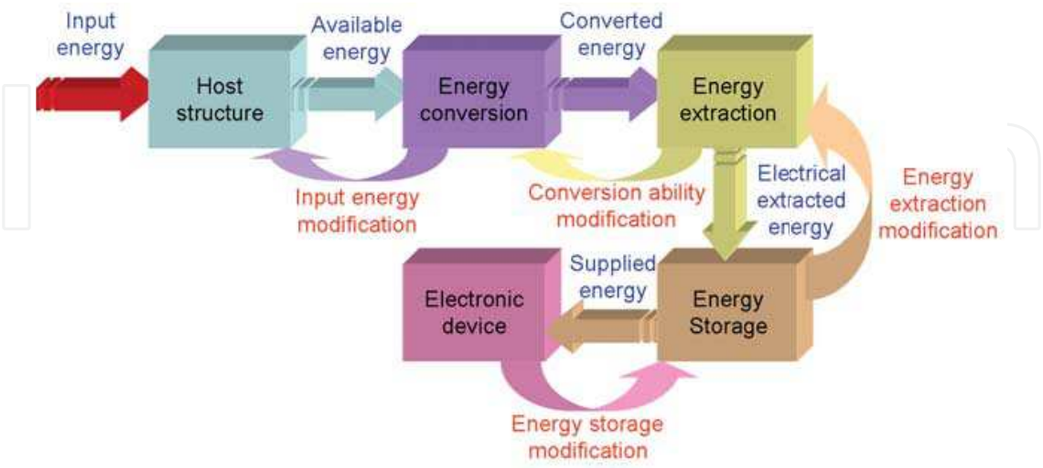

Fig. 1. General energy harvesting chain

However, the energy transfer is not unidirectional. There exist backward couplings that alter the behavior of the previous stage (Figure 1). Therefore, because of these backward couplings, the design of an efficient energy harvester should take the whole system into account. In particular, three main issues have to be considered to dispose of an effective microgenerator:

- Maximization of the energy that enters into the host structure.
- Enhancement of the conversion abilities of the material.
- Optimization of the energy transfer.

3.1 Piezoelectric system

When considering vibration energy harvesting using the piezoelectric effect, two cases can be considered. Either the piezoelectric element is directly bonded on the structure (Figure 2(a)), yielding an open-circuit piezovoltage that is a direct image of the strain and stress within the host structure, or an additional mechanical system is used (Figure 2(b)), allowing an easier maintenance but requiring a fine tuning of the resonance frequency so that it matches one of the mode of the host structure[1]. In all the cases however, the system is operating under dynamic mode in order to dispose of a significant amount of mechanical energy (Keawboonchuay and Engel, 2003).

In the case of direct coupling the energy provided by the input force is first converted into mechanical energy through the host structure, and then to electrostatic energy by the piezoelectric element, while when using indirect coupling an additional mechanical to mechanical energy conversion stage appears (a part of the energy in the host structure is transferred to the additional mechanical system).

The previous design criteria when using piezo-based microgenerators therefore consist of:

- Properly positioning the piezoelement near maximum strain/stress locations (for direct coupling) or maximum acceleration areas (for indirect coupling) and adapting the additional structure to the host structure in the case of seismic coupling.
- Using piezoelectric elements featuring high coupling coefficients and/or using artificial enhancement of the global coupling factor.
- Adapting the load seen by the piezoelectric element.

Obviously, the interdependence of the conversion stages necessitates a global approach rather than an individual optimization. A typical example is the damping effect generated by the harvesting process (Lesieutre, Ottman and Hofmann, 2003): as a significant part of the mechanical energy is converted into electricity, the former decreases, limiting the vibrations of the structure and thus the output electrical power.

(a) Direct coupling (b) Indirect (seismic) coupling

Fig. 2. Typical configurations for vibration energy harvesting using piezoelectric elements

[1] In the case of seismic coupling multimodal energy harvesting is therefore delicate.

Generally, the structure optimization consists of allowing a large amount of energy to enter in the piezoelectric element (which can be obtained by using a proper geometry - Zhu, Tudor and Beeby (2010)) and ensuring a wide frequency range operation, hence allowing energy entering whatever the force frequency is. This can be achieved by using variable resonance frequency (Challa *et al.*, 2008; Lallart, Anton and Inman, 2010b) or using nonlinear structures (Andò *et al.*, 2010; Blystad and Halvorsen, 2010a; Erturk, Hoffmann and Inman, 2009; Soliman *et al.*, 2008). Another commonly adopted solution is to use several cantilevers with different lengths (Shahruz, 2006), which however decreases the power density. The optimization of the last two items will be exposed in Sections 4 and 5.

3.2 Pyroelectric system

The case of pyroelectric energy harvesting consists of extracting energy of time-variable heat trough the thermal capacitance of the active material (Figure 3). The optimization of the input energy lies in the trade-off in the heat capacitance value, as energy should enter easily (low heat capacitance value and high thermal conductivity) and amount of available energy (high heat capacitance value).

For the conversion stage, the design is easier than in the case of piezoelectric elements, as the backward coupling can be neglected in almost all pyroelectric systems. In addition, as pyroelectric effect principles are close to those of the piezoelectric effect, the conversion enhancement and transfer optimization are similar to the case of piezo-based devices, as it will be explained in Sections 4 and 5.

4. Conversion improvement

The purpose of this section is to expose possibilities for improving the energy conversion. To introduce this concept, it is proposed to consider a piezoelectric-based system. From the equation of motion of the simple spring-mass-damper model (Eq. (3)), the energy analysis over a time period $[t_0; t_0 + T]$ is obtained by integrating in the time-domain the product of the equation by the velocity:

$$\frac{1}{2}M\left[\dot{u}^2\right]_{t_0}^{t_0+T} + \frac{1}{2}K_E\left[u^2\right]_{t_0}^{t_0+T} + C\int_{t_0}^{t_0+T}(\dot{u})^2\,dt + \alpha_u\int_{t_0}^{t_0+T}V\dot{u}dt = \int_{t_0}^{t_0+T}F\dot{u}dt, \qquad (5)$$

where all the corresponding energies are given in Table 2. Therefore it can be seen that the converted energy depends on the force factor α_u and on the time integral of the product of the voltage by the speed:

$$W_{conv}|_{piezo} = \alpha_u\int_{t_0}^{t_0+T}V\dot{u}dt. \qquad (6)$$

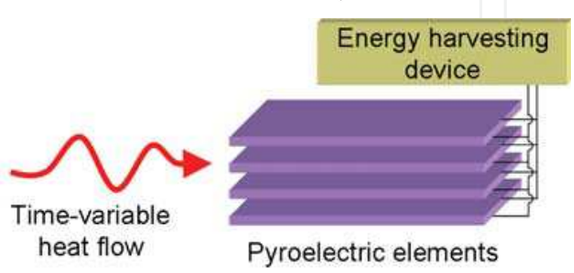

Fig. 3. Typical configuration for thermal energy harvesting using pyroelectric elements

Term	Meaning
$\frac{1}{2}M\left[\dot{u}^2\right]_{t_0}^{t_0+T}$	Kinetic energy
$\frac{1}{2}K_E\left[u^2\right]_{t_0}^{t_0+T}$	Potential energy
$C\int_{t_0}^{t_0+T}(\dot{u})^2\,dt$	Dissipated energy
$\alpha_u\int_{t_0}^{t_0+T}V\dot{u}dt$	Converted energy
$\int_{t_0}^{t_0+T}F\dot{u}dt$	Provided energy

Table 2. Definition of the energies in the case of piezoelectric energy harvesting

Such an analysis can obviously be applied to pyroelectric conversion, yielding the amount of converted energy:

$$W_{conv}|_{pyro} = \alpha_\theta \int_{t_0}^{t_0+T} V\dot{\theta}dt \tag{7}$$

Hence, in order to enhance the conversion abilities of the system, three ways can be explored:

- Increase α_u (for vibration energy harvesting) or α_θ (for thermal energy harvesting).
- Increase the voltage.
- Decrease the time shift between voltage and speed (or temperature variation rate).

Usually, the first point corresponds to the use of piezoelectric materials with higher intrinsic coupling coefficient (Rakbamrung *et al.*, 2010). This has been done recently through the use of single crystal devices (Khodayari *et al.*, 2009; Park and Hackenberger, 2002; Sun *et al.*, 2009), which typically allows increasing the harvested power by a factor of 20 (Badel *et al.*, 2006). However, single crystals are difficult to obtain, and no industrial process has been achieved, compromising the design of low-cost microgenerators using such materials.
In order to enhance the harvesting abilities, a nonlinear approach has been proposed that allows an artificial increase of the global electromechanical coupling coefficient (Guyomar *et al.*, 2005; Lefeuvre *et al.*, 2006; Makihara, Onoda and Miyakawa, 2006; Qiu *et al.*, 2009; Shu, Lien and Wu, 2007). This process consists of quickly inverting the piezoelectric voltage when the displacement or temperature reaches a maximum or a minimum value (or equivalently when the velocity cancels), as shown in Figure 4. Thanks to the dielectric behavior of piezoelectric and pyroelectric materials, the voltage is continuous. Hence, the inversion process allows a cumulative voltage increase effect, as well as an additional piecewise constant voltage that is proportional to the sign of the velocity, allowing a magnification of the energy conversion using both the voltage increase and the reduction of the time shift between voltage and velocity. Practically, the inversion of the voltage is obtained by intermittently connecting the active material to an inductor L (Figure 5), shaping a resonant network which permits the voltage inversion if the switch SW is open for half an electrical oscillation period. Nevertheless, the losses in this switching circuit lead to an imperfect inversion characterized by the inversion factor γ (corresponding to the ratio between absolute voltages after and before the inversion), which is comprised between 0 (no inversion - voltage cancellation) and 1 (perfect inversion).
In the framework of energy harvesting, the switching element can be placed either in parallel or in series with the classical energy harvesting circuit (which consists of connecting the material to a diode rectifier bridge and a smoothing capacitor C_s as shown in Figure 6(a)), respectively leading to the principles of the parallel *Synchronized Switch Harvesting on Inductor*

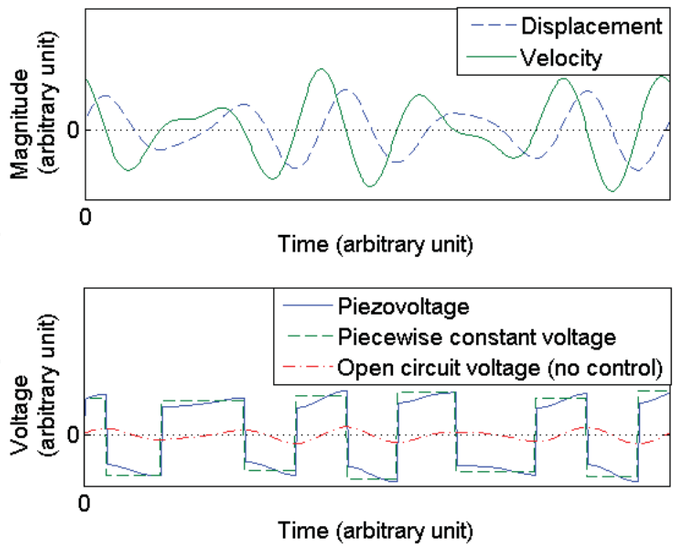

Fig. 4. Nonlinear treatment principles

Fig. 5. Practical implementation of the voltage inversion technique

(parallel SSHI - Figure 6(b) - Guyomar *et al.* (2005)) and series *Synchronized Switch Harvesting on Inductor* (series SSHI - Figure 6(c) - Lefeuvre *et al.* (2006); Taylor *et al.* (2001)). Such an approach typically allows a gain of 10 using classical components compared to the classical technique when considering constant displacement magnitude. Harvested energies as a function of the systems parameters (with f_0 the vibration frequency, X_M the displacement or temperature variation magnitude and R_L the equivalent connected load) are listed in Table 3.
However, backward coupling influences the mechanical behavior of the host structure (more particularly by introducing a damping effect) when using piezoelectric energy harvesting at the resonance frequency. In this case, it is possible to get the displacement magnitude u_M from the mechanical energy analysis of the system, leading to the normalized harvested

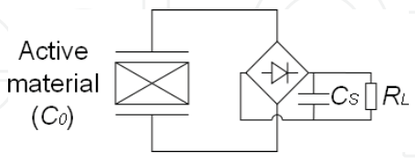

(a) Classical

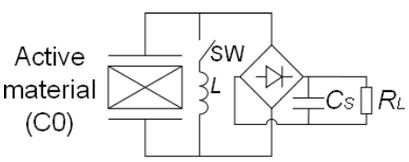

(b) Parallel SSHI

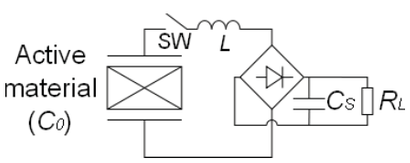

(c) Series SSHI

Fig. 6. Energy harvesting circuits

Technique	Harvested energy	Maximal harvested energy	Gain ($\gamma = 0.8$)
Standard	$\frac{(4\alpha f_0)^2 R_L}{(1+4R_L C_0 f_0)^2} {X_M}^2$	$\frac{\alpha^2}{C_0} f_0 {X_M}^2$	–
Parallel SSHI	$\frac{(4\alpha f_0)^2 R_L}{[1+2(1-\gamma)R_L C_0 f_0]^2} {X_M}^2$	$\frac{2}{1-\gamma}\frac{\alpha^2}{C_0} f_0 {X_M}^2$	10
Series SSHI	$\frac{[4(1+\gamma)\alpha f_0]^2 R_L}{[(1-\gamma)+4(1+\gamma)R_L C_0 f_0]^2} {X_M}^2$	$\frac{1-\gamma}{1-\gamma}\frac{\alpha^2}{C_0} f_0 {X_M}^2$	9

Table 3. Harvested energies for classical and SSHI techniques and gain under constant displacement magnitude

powers depicted in Figure 7. To make this chart as independent as possible from the system parameters, the power has been normalized with respect to the maximal harvested power in the standard case when taking into account the damping effect:

$$P_{lim} = \frac{{F_M}^2}{8C}, \tag{8}$$

with F_M the driving force magnitude. The x-axis of Figure 7 corresponds to the figure of merit given by the product of the squared global coupling coefficient k^2 (reflecting the amount of energy that can be converted) by the mechanical quality factor Q_M (giving an image of the effective available energy). This figure shows that the standard and SSHI techniques feature the same power limit, but the nonlinear approaches permit harvesting the same amount of energy than the classical scheme for much lower values of $k^2 Q_M$, meaning that much less volume of active materials is required. Figure 7 also shows that the series SSHI performance is very close to the parallel SSHI. It can be noted that these nonlinear approaches also permit increasing the bandwidth of the microgenerator (Lallart *et al.*, 2010c). Losses in the inductance that limit the power increase can also be controlled using proper approaches, such as smoother inversion (Lallart *et al.*, 2010d), PWM actuation that insures a perfect inversion[2] (Liu *et al.*, 2009) or by ensuring that the inversion losses are always less than the converted energy over a given time period (Guyomar and Lallart, 2011).

Finally, another way to enhance the conversion abilities is to consider a bidirectional energy flow from the source to the storage stage (Lallart and Guyomar, 2010e). This approach permits beneficiating of a particular "energy resonance" effect as the converted energy equals the

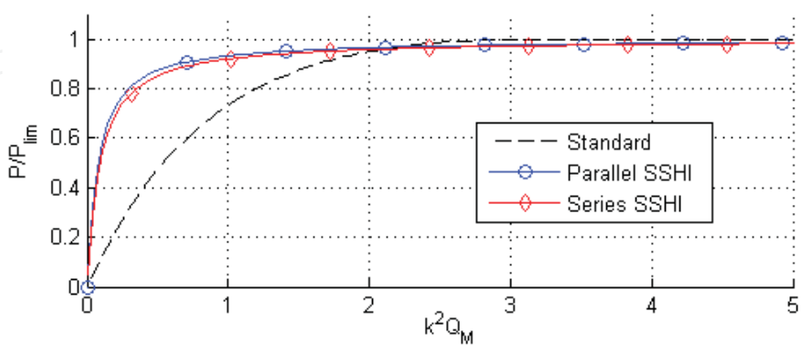

Fig. 7. Normalized harvested powers under constant force magnitude at the resonance frequency

[2] In this case, driving losses may however compromise the energy balance.

converted energy without providing initial energy (from the storage stage) plus twice the cross-product of the initial voltage V_0 times the voltage generated by the active material:

$$W_{conv}|_{bidir} = \frac{1}{2}C_0\left(\frac{\alpha}{C_0}X_M + V_0\right)^2 - \frac{1}{2}C_0{V_0}^2 = \frac{1}{2}\left[\frac{\alpha^2}{C_0}{X_M}^2 + 2\alpha V_0 X_M\right]. \quad (9)$$

Hence, as the harvested energy increases, the initial provided energy during the beginning of a new cycle increases as well, allowing harvesting more energy, and therefore closing the "energy resonance" loop. This approach permits a typical harvested energy gain up to 40 under constant displacement magnitude (or constant temperature variation magnitude) as well as bypassing the power limit when considering the damping effect.
It can also be noticed that instead of adding external nonlinearities, Guyomar, Pruvost and Sebald (2008); Khodayari *et al.* (2009); Zhu *et al.* (2009) have shown that the energy harvesting performance may be also enhanced by using the intrinsic nonlinear behaviors of pyroelectric materials, such as ferroelectric↔ferroelectric or ferroelectric↔paraelectric phase transitions.

5. Energy transfer optimization

The next stage in the energy conversion chain lies in the energy transfer from the active material to the storage stage. As the amount of energy provided to the electronic device may alter the energy conversion process (which can be seen from the load-dependent powers in Table 3 and in Figure 8), additional interfaces have to be included so that the energy extracted from the active material is maximum. This section proposes to expose two possibilities to ensure a harvested energy independent from the connected load by:

- Ensuring that the active material sees the optimal load.
- Decoupling the extraction and storage stage through a nonlinear approach.

The simplest way for ensuring that the load seen by the piezoelectric or pyroelectric material equals the optimal one that maximizes the harvested power consists of adding a converter between the active element and the extraction stage (Han *et al.*, 2004; Lallart and Inman,

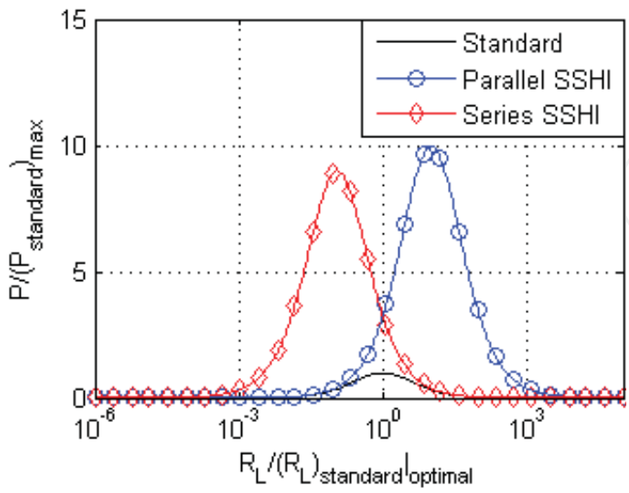

Fig. 8. Normalized harvested powers under constant displacement magnitude (or constant temperature variation magnitude) as a function of the load (normalized with respect to the optimal load in the standard case)

2010f; Lefeuvre *et al.*, 2007a; Ottman *et al.*, 2002; Ottman, Hofmann and Lesieutre, 2003). The converter should operate in discontinuous mode in order to present a constant (or almost constant) impedance to the piezoelectric element. Usually, the converter parameter (inductance L, switching frequency f_{sw} and duty cycle δ) should also be tuned so that its input impedance is close to the optimal load that maximizes the extracted energy (Table 4)[3], although an automatic detection of the optimal operating point can be done (Lallart and Inman, 2010f; Ottman *et al.*, 2002).

Another approach for ensuring a harvested energy independent from the load consists of slightly modifying the previously exposed nonlinear techniques. In particular, if the switching time period is reduced so that it stops when the voltage across the active material is zero, all the electrostatic energy available on the material is transferred to the inductance (under magnetic form). If this energy can then be transferred to the load, there would not be any direct connection between the load and the piezoelectric or pyroelectric material, thus allowing a decoupling between the energy extraction stage and the energy storage stage. Such a technique, called *Synchronous Electric Charge Extraction* (Lefeuvre *et al.*, 2005; 2006), is depicted in Figure 9. The SECE approach also permits an enhancement of the conversion thanks to a voltage increase and a reduction of the time shift between voltage and velocity, and allows a typical energy gain of 3.5 compared to the maximal harvested energy in the standard case under constant displacement magnitude.

Nevertheless, the SECE techniques does not allow controlling the trade-off between extracted energy and conversion improvement, as all the energy on the active material is extracted. The principles of the technique may be enhanced by combining the series SSHI approach with the SECE, leading to the DSSH technique (Lallart *et al.*, 2008a). This scheme, depicted in Figure 10, consists in first extracting a part of the electrostatic energy on the piezoelectric or pyroelectric material on an intermediate capacitor C_{int}, while the remaining energy is used to perform the voltage inversion leading to the conversion magnification. Then the energy available on the intermediate capacitor is transferred to the load in the same way than the SECE. Hence, through the ratio between the active element capacitance and intermediate capacitance, it is possible to finely control the trade-off between extracted energy and conversion enhancement, allowing a typical harvested energy 7.5 higher than the maximal harvested energy in the

Type	Impedance	Efficiency
Step-down (Ottman, Hofmann and Lesieutre, 2003)	$\left(\frac{2Lf_{sw}}{\delta^2}\right)\left(\frac{1}{1-\frac{V_{out}}{V_{in}}}\right)$	65%
Buck-boost (Lefeuvre *et al.*, 2007a)	$\left(\frac{2Lf_{sw}}{\delta^2}\right)$	75%

Table 4. Impedance matching systems (V_{out} and V_{in} refer to output and input voltages)

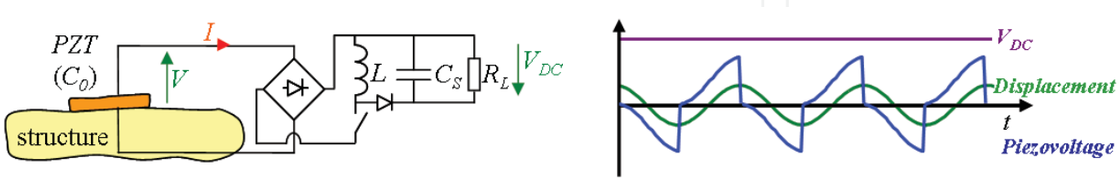

Fig. 9. SECE technique

[3] As the optimal load depends on the frequency, broadband energy harvesting is quite delicate for these architectures.

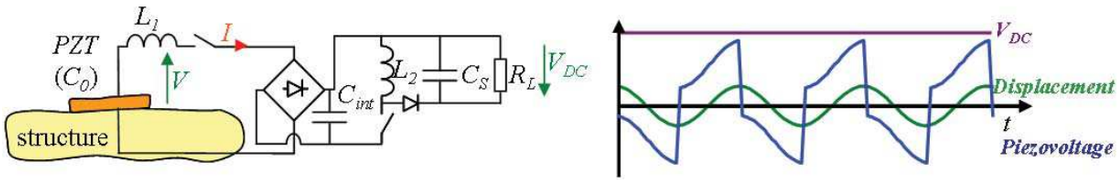

Fig. 10. DSSH technique

standard case under constant displacement magnitude or constant temperature variation magnitude and independent from the connected load. The SECE and DSSH techniques have also the advantage of being able to harvest energy even for low load values, while in the case of low frequency (typical for temperature variation), the optimal load for the standard and SSHI approaches would be very large.

When taking into account the damping effect caused by the backward coupling in the case of mechanical energy harvesting using piezoelectric principles, the harvested energy using the SECE and DSSH techniques is given in Table 5 and depicted in Figure 11.

Figure 11 shows the effectiveness of the techniques for allowing a significant power output even for low values of the figure of merit k^2Q_M, especially for the DSSH approach, which permits the same power output than the standard technique with 10 times less active materials. Contrarily to the SECE technique, the DSSH does not present a decreasing power for large values of k^2Q_M as the intermediate capacitor also permits controlling the trade-off between extracted energy and damping effect (or equivalently the backward coupling between energy conversion stage and host structure). It can be noted that, due to the losses in the inductance during the energy transfer process, the power limit is decreased.

Technique	Harvested energy	
SECE	$\gamma_C \frac{2}{\pi} \frac{k^2Q_M}{\left(1+\frac{4}{\pi}k^2Q_M\right)^2} \frac{{F_M}^2}{C}$	
DSSH[4]	$\gamma_C \frac{2\pi k^2Q_M(1-\gamma)^2}{(\pi(1-\gamma)+4k^2Q_M(1+\gamma))^2} \frac{{F_M}^2}{C}$	for $k^2Q_M \leq \frac{4}{\pi}\frac{1-\gamma}{1+\gamma}$
	$\gamma_C \frac{{F_M}^2}{8C}$	for $k^2Q_M \geq \frac{4}{\pi}\frac{1-\gamma}{1+\gamma}$

Table 5. Harvested energies for SECE and DSSH techniques under constant force magnitude (γ_C refers to the energy transfer efficiency)

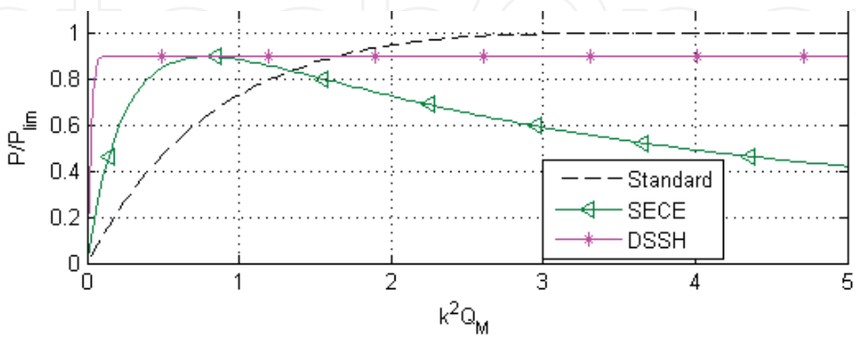

Fig. 11. Harvested energy for the SECE and DSSH techniques ($\gamma_C = 0.9$)

[4] for the optimal intermediate capacitance value

However, this statement has to be weighted by the fact that classical and SSHI approaches require load adaptation stages, whose effectiveness is usually less than 80%. Hence, the power limit of the SECE and DSSH schemes is similar to the one obtained with the other techniques featuring load adaptation stages. Such a statement also applies for constant vibration magnitude or constant temperature variation magnitude case. Finally, it can be noted that the power transfer from the intermediate capacitor to the load can also be controlled by fixing a voltage threshold value, leading to the concept of *Enhanced Synchronized Switch Harvesting* (ESSH) described by Shen *et al.* (2010).

6. Implementation considerations

Now the general principles of energy harvesting exposed, it is proposed in this section to discuss about their implementation for the design of realistic self-powered devices.

The first issue that may arise for the use of nonlinear techniques is the control of the switching device. Actually, the minimum and maximum detection can be done by comparing the voltage across the active material with its delayed version. The maximum is then detected when the delayed signal is greater than the original one (Lallart *et al.*, 2008b; Liang and Liao, 2009; Qiu *et al.*, 2009; Richard, Guyomar and Lefeuvre, 2007). The self-powered autonomous switching device based on this principles therefore consumes very little power, typically less than 5% than the electrostatic energy available on the ferroelectric material, therefore not compromising the energy harvesting gain. The implementation of the self-powered switch, depicted in Figure 12, also shows that only typical electronic components are required, allowing an easy integration of the device.

Another point of interest when designing realistic energy harvesters is the incoming solicitation. While sine excitation is usually considered for theoretical analysis, realistic systems would be more likely subjected to random input (Blystad, Halvorsen and Husa, 2010b; Halvorsen, 2008). Although very few studies addressed this problem in the case of nonlinear energy harvesting (Badel *et al.*, 2005; Lallart, Inman and Guyomar, 2010g; Lefeuvre *et al.*, 2007b), it can be stated that load independent techniques (SECE, DSSH and ESSH) would be more suitable under such circumstance, as the optimal load is frequency-dependent for the other approaches.

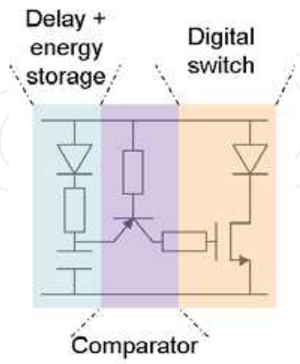

Fig. 12. Principles of the self-powered switch for maximum detection (the minimum detection is simply obtained by reversing the polarity of the system)

Finally, one of the most promising applications of ferroelectric materials used for energy harvesting lies in the MEMS[5] scale. However, when dealing with electroactive microsystems, the output voltage that can be expected is quite low. This may be a serious issue when dealing with energy harvesting as energy harvesting interfaces feature discrete components such as diodes or transistors that present voltage gaps due to their semiconductor nature, hence compromising the operations of the microgenerators. In order to counteract this drawbacks, it is possible to replace the inductance of the series SSHI by a transformer in order to divide the threshold voltage of diodes seen by the piezoelectric element (Garbuio *et al.*, 2009), or to use mechanical rectifiers (Nagasawa *et al.*, 2008).

7. Application examples

In this section two examples of self-powered devices will be exposed, demonstrating the possibility of designing systems powered up by their close environment. However, a careful attention has to be placed on the power management strategy, in order to have a positive energy balance between harvested energy and supplied energy. Some general design rules can be considered for saving energy:

- Use sleep modes as much as possible.
- Optimize components that require the highest energy per operating cycle, rather than devices consuming the highest power. For example, a system that consumes 1 mW for 10 μs (hence necessitating 10 nJ) is therefore less critical than a device requiring 10 μW for 1 s, as the associated energy per cycle of the latter is 10 μJ.
- Re-think the processes to minimize the energy.

7.1 Self-powered accelerometer

The first proposed application example is a self-powered accelerometer. The system is composed by a SSHI energy harvesting device, a microcontroller (for power management, data acquisition and communication management), a low-power accelerometer followed by a filter to obtain the average acceleration and a RF module for data transmission (Figure 13).
When the harvested energy is sufficient (approximately 1 mJ), the microcontroller wakes up and enables the accelerometer as well as the RF transmission module. After a predefined wake-up time, the filtered output signal of the latter is digitized by the microcontroller. The measurement results are then sent by RF transmission together with an identifier. The accelerometer and RF module are finally turned off and the microcontroller enters in sleep

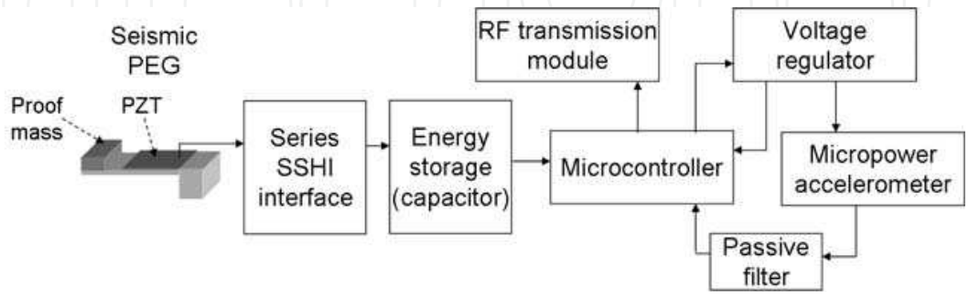

Fig. 13. Architecture of the self-powered accelerometer

[5] *Micro Electro-Mechanical Systems*

mode. If the energy is still sufficient, a new cycle is repeated after a given time period (typically 10 s). The obtained waveforms using this device are depicted in Figure 14.

7.2 Self-powered SHM system

The second autonomous, self-powered wireless system presented in this section lies in a *in-situ* structural condition monitoring system (Figure 15), which consists in analyzing the interaction of an acoustic wave (Lamb wave) with the host structure (Guyomar *et al.*, 2007; Lallart *et al.*, 2008c). The device is made of two self-powered components (Figure 16):

- The *Autonomous Wireless Transmitter* (AWT), which consists in harvesting energy with the SSH module, and when the latter is sufficient, a microcontroller wakes up and applies a pulse voltage on a additional piezoelectric element, which therefore generates the Lamb wave. Then the AWT sends a RF signal containing its identifier for time and space localization before entering into sleep mode for a given time period.
- The *Autonomous Wireless Receiver* (AWR), which also includes a SSHI system. The AWR features a RF listening module which wakes up the system when it senses a RF

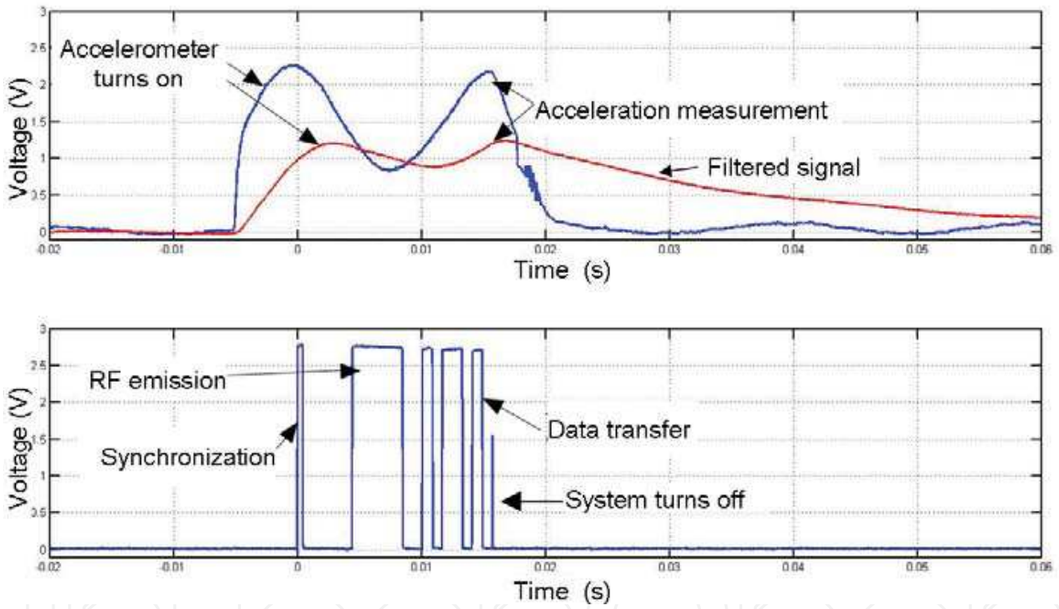

Fig. 14. Waveforms of acceleration measurements and RF comunication

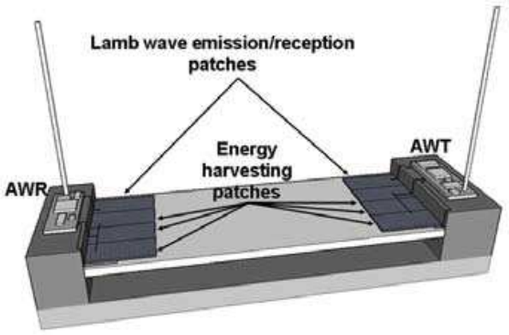

Fig. 15. Self-powered SHM system

(a) AWT (b) AWR

Fig. 16. Structures of the self-powered SHM subsystems

communication incoming from a close AWT. Once woken up, the Lamb wave signature is sensed, amplified, and its RMS value computed. This value is then compared to a reference value (obtained in the pristine case), allowing the estimation of the change in the mechanical structure. The results are then sent by RF transmission together with an identifier. Once these operations terminated, the whole system enters into sleep mode. After a predefined time period, the RF listening module is enabled to detect a new inspection cycle.

In addition, an externally powered base station is used to gather the data. A summary of the communication within the network is depicted in Figure 17 and the energy balance of the system as a function of the stress within the structure is presented in Table 6. The energy consumption estimation for the AWT and AWR are given by:

AWT :

- Microcontroller wake-up: 0.8 mJ
- RF emission: 0.2 mJ
- Lamb wave emission: 0.2 mJ

Total: 1.20 **mJ**

AWR :

- Microcontroller wake-up: 0.8 mJ
- RF listening: 0.6 mJ (average listening time: 3 s)
- Damage Index computation: 0.03 mJ
- RF emission: 0.25 mJ

Total: 1.68 **mJ**

According to Table 6, the system can operate as soon as the stress reaches 2 MPa, which is a realistic stress value in classical structures. It can also be noted that the AWR energy scavenging device features higher global coupling coefficient than the AWT, allowing to harvest more energy in a given time period.
The damage detection estimation has been investigated by adding an artificial damage consisting in a small mass of putty on the structure. Waveforms depicted in Figure 18 demonstrate the ability of the proposed system for quantitatively detecting the change in the structural condition.

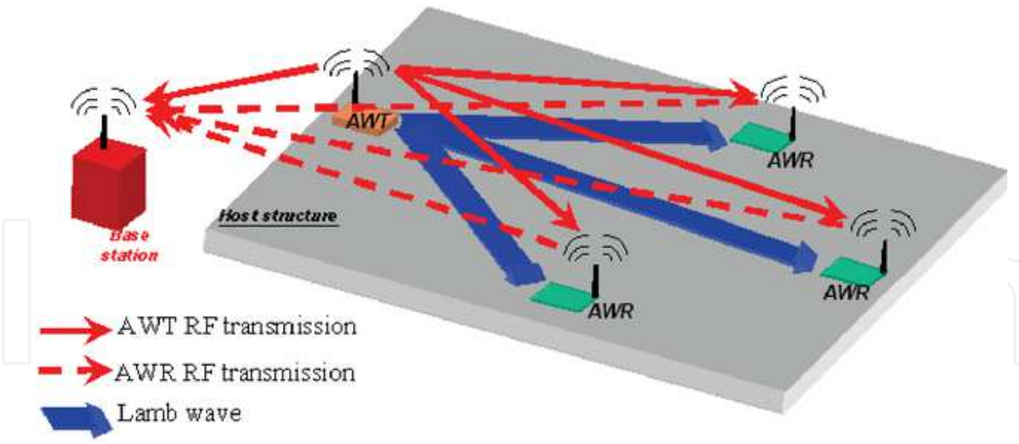

Fig. 17. Communication network for the self-powerd SHM system

Stress (*MPa*)	1.5	1.75	2	2.25	2.5	3	3.5
Harvested energy in 10 s (mJ) for the AWT	0.77	1.05	1.36	1.72	2.13	3.06	4.17
Harvested energy in 10 s (mJ) for the AWR	1.10	1.5	1.96	2.48	3.06	4.41	6.00
Energy balance (mJ) for the AWT	−0.43	−0.15	0.16	0.52	0.93	1.86	2.97
Energy balance (mJ) for the AWR	−0.58	−0.18	0.28	0.80	1.38	2.73	4.32

Table 6. Energy balance for the self-powered wireless SHM device

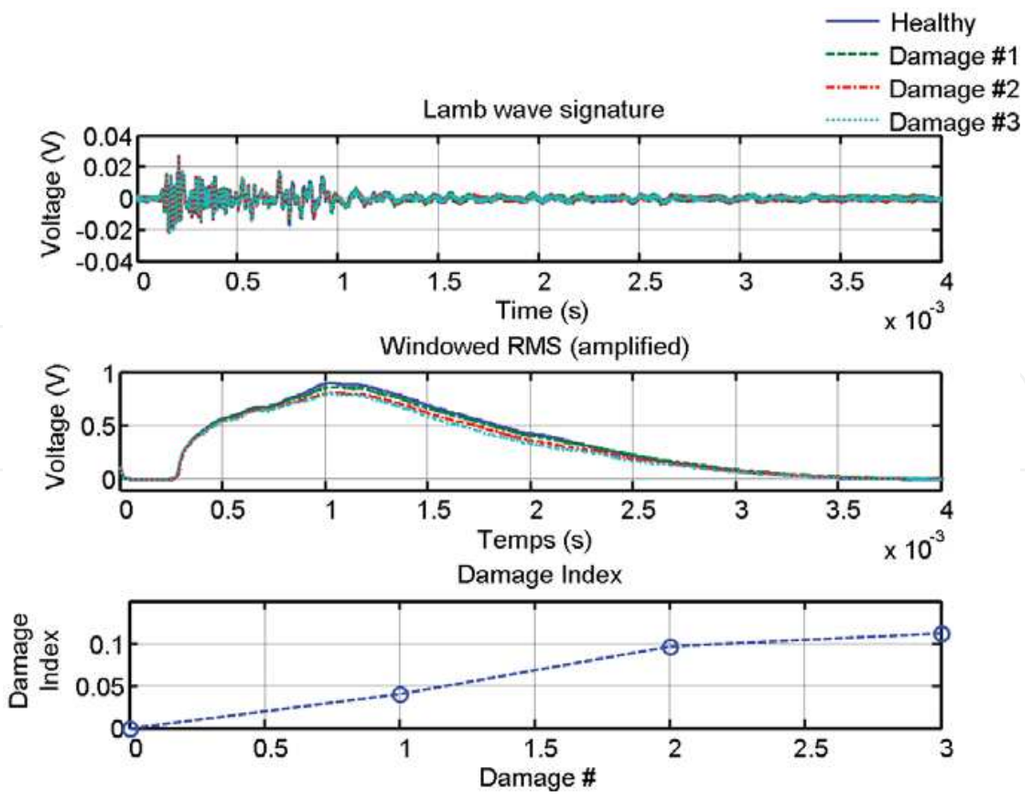

Fig. 18. Results of the self-powered SHM system under artificial damage.

8. Conclusion

This chapter exposed the application of ferroelectric materials to small-scale energy scavenging devices and self-powered systems, with a special focus on vibrations and temperature variations, as ferroelectric devices present high energy densities and promising integration potentials. From the analysis of the global energy transfer chain from the energy source to the device to power up, it has been shown that the design of efficient microgenerators has to be done in a global manner rather than optimizing each block independently, because of backward couplings to may modify the behavior of previous stages. Then several ways for improving the performance of energy harvesters have been explored, showing that the use of nonlinear approaches may significantly increase the energy conversion abilities and/or the independency from the connected device. Fundamental issues such as realistic implementation, performance under real excitation and microscale design have then been discussed. Finally, the possibility of designing truly self-powered wireless systems has been demonstrated through two working application examples, showing that the spreading of devices powered up by energy harvested from their close environment is now only a question of time.

9. References

Andò, B.; Baglio, S.; Trigona, C.; Dumas, N.; Latorre, L. & Nouet, P. (2010). Nonlinear mechanism in MEMS devices for energy harvesting applications. *Smart Mater. Struct.*, Vol. 20, 125020.

Anton, S. R. & Sodano H. A. (2007). A review of power harvesting using piezoelectric materials (2003-2006). *Smart Mater. Struct.*, Vol. 16(3), R1-R21.

Badel, A.; Guyomar, D.; Lefeuvre, E. & Richard, C. (2005). Efficiency Enhancement of a Piezoelectric Energy Harvesting Device in Pulsed Operation by Synchronous Charge Inversion. *J. Intell. Mater. Syst. Struct.*, Vol. 16, 889-901.

Badel, A.; Benayad, A.; Lefeuvre, E.; Lebrun, L.; Richard, C. & Guyomar, D. (2006a). Single Crystals and Nonlinear Process for Outstanding Vibration Powered Electrical Generators. *IEEE Trans. on Ultrason., Ferroelect., Freq. Contr.*, Vol. 53, 673-684.

Badel, A.; Lagache, M.; Guyomar, D.; Lefeuvre, E. & Richard, C. (2007). Finite Element and Simple Lumped Modeling for Flexural Nonlinear Semi-passive Damping. *J. Intell. Mater. Syst. Struct.*, Vol. 18, 727-742.

Beeby, S. P.; M. J.; & White, N. M. (2006). Energy harvesting vibration sources for microsystems applications, *Meas. Sci. Technol.*, Vol. 17, R175-R195.

Blystad, L.-C. J. & Halvorsen, E. (2010a). A piezoelectric energy harvester with a mechanical end stop on one side. *Microsyst. Technol., in press - available online*. DOI: DOI: 10.1007/s00542-010-1163-0.

Blystad, L.-C. J.; Halvorsen, E. & Husa, S. (2010b). Piezoelectric MEMS energy harvesting systems driven by harmonic and random vibrations. *IEEE Trans. Ultrason., Ferroelect., Freq. Contr.*, Vol. 57(4), 908-919.

Challa, V. R.; Prasad, M. G.; Shi, Y. & Fisher, F. T. (2008). A vibration energy harvesting device with bidirectional resonance frequency tunability. *Smart Mater. Struct.*, Vol. 17, 015035.

Erturk A. & D. J. Inman (2008). Issues in mathematical modeling of piezoelectric energy harvesters. *Smart Mater. Struct.*, Vol. 17, 065016.

Erturk A.; Hoffmann, J. & D. J. Inman (2010). A piezomagnetoelastic structure for broadband vibration energy harvesting. *Appl. Phys. Lett.*, Vol. 94, 254102.

Garbuio, L.; Lallart, M.; Guyomar, D. & Richard, C. (2009). Mechanical Energy Harvester with Ultra-Low Threshold Rectification Based on SSHI Non-Linear Technique, *IEEE Trans. Indus. Elec.*, Vol. 56(4), 048-1056.

Guyomar, D.; Badel, A.; Lefeuvre, E. & Richard, C. (2005). Towards energy harvesting using active materials and conversion improvement by nonlinear processing, *IEEE Trans. Ultrason., Ferroelect., Freq. Contr.*, Vol. 52, 584-595.

Guyomar, D.; Jayet, Y.; Petit, L.; Lefeuvre, E.; Monnier, T.; Richard, C. & Lallart, M. (2007). Synchronized Switch Harvesting applied to Self-Powered Smart Systems : Piezoactive Microgenerators for Autonomous Wireless Transmitters, *Sens. Act. A: Phys.*, Vol. 138, No. 1, 151-160.

Guyomar, D.; Pruvost, S. & Sebald, G. (2008). Energy Harvesting Based on FE-FE Transition in Ferroelectric Single Crystals, *IEEE Trans. Ultrason., Ferroelect., Freq. Contr.*, Vol. 55(2), 279-285.

Guyomar, D.; Sébald, G.; Pruvost, S.; Lallart, M.; Khodayari, A. & Richard, C. (2009). Energy Harvesting From Ambient Vibrations and Heat, *J. Intell. Mater. Syst. Struct.*, Vol. 20(5), 609-624.

Guyomar, D. & Lallart, M. (2011). Switching loss reduction in Nonlinear Piezoelectric Conversion under Pulsed Loading, *IEEE Trans. Ultrason., Ferroelect., Freq. Contr.*, Vol. 58(3), 494-502.

Halvorsen, E. (2008). Energy Harvesters Driven by Broadband Random Vibrations. *J. Microelectromech. Syst.*, Vol. 17(5), 1061-1071.

Han, J.; Von-Jouanne,A.; Le, T.; Mayaram, K. & Fiez, T. S. (2004). Novel power conditioning circuits for piezoelectric micro power generators. In *Proc. IEEE Appl. Power Electron. Conf. Expo. (APEC)*, vol. 3, 1541-1546.

Hudak, N. S. & Amatucci, G. G. (2008). Small-scale energy harvesting through thermoelectric, vibration, and radiofrequency power conversion. *Appl. Phys. Rev.*, Vol. 103, 101301.

Jia, D. & Liu, J (2009). Human power-based energy harvesting strategies for mobile electronic devices. *Front. Energy Power Eng. China*, Vol. 3(1), 27Ú46.

Keawboonchuay , C. & Engel, T. G. (2003). Electrical power generation characteristics of piezoelectric generator under quasi-static and dynamic stress conditions. *IEEE Trans. Ultrason., Ferroelect., Freq. Contr.*, Vol. 50, 1377-1382.

Khodayari, A.; Pruvost, S.; Sebald, G.; Guyomar, D. & Mohammadi, S. (2009). Nonlinear Pyroelectric Energy Harvesting from Relaxor Single Crystals. *IEEE Trans. Ultrason., Ferroelect., Freq. Contr.*, Vol. 56(4), 693-699.

Krikke, J. (2005). Sunrise for energy harvesting products. *IEEE Pervasive Comput.*, Vol. 4, 4-35.

Lallart, M.; Garbuio, L.; Petit, L.; Richard, C. & Guyomar, D. (2008a) Double Synchronized Switch Harvesting (DSSH) : A New Energy Harvesting Scheme for Efficient Energy Extraction, *IEEE Trans. Ultrason., Ferroelect., Freq. Contr.*, Vol. 55,(10), 2119-2130.

Lallart, M.; Lefeuvre, E.; Richard, C. & Guyomar, D. (2008b). Self-Powered Circuit for Broadband, Multimodal Piezoelectric Vibration Control. *Sens. Act. A: Phys.*, Vol. 143, No. 2, 277-382, 2008.

Lallart, M.; Guyomar, D.; Jayet, Y.; Petit, L.; Lefeuvre, E.; Monnier, T.; Guy, P. & Richard, C. (2008c). Synchronized Switch Harvesting applied to Selfpowered Smart Systems: Piezoactive Microgenerators for Autonomous Wireless Receiver, *Sens. Act. A: Phys.*, Vol. 147, No. 1, 263-272.

Lallart, M. (2010a). Conversion électroactive et application aux systèmes auto-alimentés[6]. Editions Universitaires Européennes, *in french*. ISBN: 978-613-1-50507-2

Lallart, M.; Anton, S. R. & Inman, D. J. (2010b). Frequency Self-tuning Scheme for Broadband Vibration Energy Harvesting. *J. Intell. Mat. Syst. Struct.*, Vol. 21(9), 897-906 .

Lallart, M.; Guyomar, D.; Richard, C. & Petit, L. (2010c). Nonlinear optimization of acoustic energy harvesting using piezoelectric devices. *J. Acoust. Soc. Am.*, Vol. 128(5), 2739-2748.

Lallart, M.; Garbuio, L; Richard, C. & Guyomar, D. (2010d). High Efficiency, Low-Cost Capacitor Voltage Inverter for Outstanding Performances in Piezoelectric Energy Harvesting, *IEEE Trans. on Ultrason., Ferroelect., Freq. Contr.*, Vol. 57(2), 281-291.

Lallart, M. & Guyomar, D. (2010e). Piezoelectric conversion and energy harvesting enhancement by initial energy injection. Appl. Phys. Lett., Vol. 97, # 014104.

Lallart, M. & Inman, D. J. (2010f). Low-Cost Integrable Tuning-Free Converter for Piezoelectric Energy Harvesting Optimization. *IEEE Trans. Power Electron.*, Vol. 25(7), 1811-1819.

Lallart, M.; Inman, D. J. & Guyomar, D. (2010g). Transient Performance of Energy Harvesting Strategies under Constant Force Magnitude Excitation. *J. Intell. Mater. Syst. Struct.*, Vol 21(13), 1279-1291.

Lefeuvre, E.; Badel, A.; Richard, C. & Guyomar, D. (2005). Piezoelectric energy harvesting device optimization by synchronous electric charge extraction. *J. Intell. Mat. Syst. Struct.*, Vol. 16, No. 10, 865-876.

Lefeuvre, E.; Badel, A.; Richard, C.; Petit, L. & Guyomar, D. (2006). A comparison between several vibration-powered piezoelectric generators for standalone systems, *Sens. Act. A: Phys*, Vol. 126, 405-416.

Lefeuvre, E.; Audigier, D.; Richard, C. & Guyomar, D. (2007a). Buck-boost converter for sensorless power optimization of piezoelectric energy harvester. *IEEE Trans. Power Electron.*, Vol. 22(5), 2018-2025.

Lefeuvre, E.; Badel, A.; Richard, C. & Guyomar, D. (2007b). Energy harvesting using piezoelectric materials: Case of random vibrations. *J. Electrocem.*, Vol. 19(4), 349-355.

Lesieutre, G. A.; G.K. Ottman, G. K. & Hofmann, H. F. (2003). Damping as a result of piezoelectric energy harvesting. *J. Sound Vib.*, Vol. 269(3-5), 991-1001.

Liang, J. R. & Liao, W. H. (2009). An Improved Self-Powered Switching Interface for Piezoelectric Energy Harvesting. In *Proc. of 2009 IEEE International Conference on Information and Automation*, 945-950.

Liu, Y.; Tian, G.; Wang, Y; Lin, J.; Zhang, Q. & Hofmann, H. F. (2009). Active Piezoelectric Energy Harvesting: General Principles and Experimental Demonstration. *J. Intell. Mat. Syst. Struct.*, Vol. 20, 575-585.

Makihara, K.; Onoda, J. & Miyakawa, T. (2006). Low energy dissipation electric circuit for energy harvesting. *Smart Mater. Struct.*, Vol. 15, 1493-1498.

Nagasawa, S.; Suzuki, T.; Takayama, Y.; Tsuji, K. & Kuwano, H. (2008). Mechanical rectifier for micro electric generators. *IEEE 21st International Conference on Micro Electro Mechanical Systems*, Tucson, AZ, USA, January 2008, 992-995.

Ottman, G. K.; Hofmann, H. F.; Bhatt, A. C. & Lesieutre, G. A. (2002). Adaptive Piezoelectric Energy Harvesting Circuit for Wireless Remote Power Supply. *IEEE Trans. Power Electron.*, vol. 17(5), 669-676.

[6] *Electroactive conversion and application to self-powered systems*

Ottman, T. S.; Hofmann, H. F. & Lesieutre, G. A. (2003). Optimized piezoelectric energy harvesting circuit using step-down converter in discontinuous conduction mode. *IEEE Trans. Power Electron.*, Vol. 18(2), 696-703.

Paradiso, J. A. & Starner, T. (2005). Energy scavenging for mobile and wireless electronics. *IEEE Pervasive Computing*, Vol. 4, 18-27.

Park, S.-E. & Hackenberger, W. (2002). High performance single crystals, applications and issues. *Current Opinion in Solid State and Material Science*, Vol. 6, 11-18.

Qiu, J.; Jiang, H.; Ji, H. & Zhu, K. (2009). Comparison between four piezoelectric energy harvesting circuits. *Front. Mech. Eng. China*, Vol. 4(2), 153-159.

Rakbamrung, P.; Lallart, M.; Guyomar, D.; Muensit, N.; Thanachayanont, C.; Lucat, C.; Guiffard, B.; Petit, L. & Sukwisut, P. (2010). Performance Comparison of PZT And PMN-PT Piezoceramics for Vibration Energy Harvesting. *Sens. Act. A: Phys.*, Vol. 163, 493-500.

Richard C.; Guyomar, D. & Lefeuvre, E. (2007). Self-Powered Electronic Breaker With Automatic Switching By Detecting Maxima Or Minima Of Potential Difference Between Its Power Electrodes, *patent # PCT/FR2005/003000*, publication number: WO/2007/063194, 2007.

Roundy, S.; Wright, P. K. & Rabaey, J. (2003). A study of low level vibrations as a power source for wireless sensor nodes. *Comp. Comm.*, Vol. 26, 1131-1144.

Shahruz, S. M. (2006). Design of mechanical band-pass filters for energy scavenging. *J. Sound Vib.*, Vol. 292, 987-998.

Shen, H.; Qiu, J.; Ji, H.; Zhu, K. & Balsi, M. (2010). Enhanced synchronized switch harvesting: a new energy harvesting scheme for efficient energy extraction. *Smart Mater. Struct.*, Vol. 20, 115017.

Shu, Y. C.; Lien, I. C. & Wu, W. J. (2007). An improved analysis of the SSHI interface in piezoelectric energy harvesting. *Smart Mater. Struct.*, Vol. 16, 2253-2264.

Soliman, M. S. M.; Abdel-Rahman, E. M.; El-Saadany, E. F.& Mansour, R. R. (2008). A wideband vibration-based energy harvester. *J. Micromech. Microeng.*, Vol 18, 115021.

Sun, C.; Qin, L.; Li, F.; Wang, Q.-M. (2009). Piezoelectric Energy Harvesting using Single Crystal $Pb(Mg_{1/3}Nb_{2/3})O_3 - xPbTiO_3$ (PMN-PT) Device. *J. Intell. Mat. Syst. Struct.*, Vol. 20(5), 559-568.

Taylor, G. W.; Burns, J. R.; Kammann, S. M.; Powers, W. B. & Welsh, T. R. (2001). The Energy Harvesting Eel: A Small Subsurface Ocean/River Power Generator. *IEEE J. Oceanic Eng.*, Vol. 26, 539-547.

Vullers, R.J.M.; van Schaijk, R.; Doms, I.; Van Hoof, C. & R. Mertens (2009). Micropower energy harvesting. *Solid-State Electronics*, Vol. 53, 684-693.

Zhu, D.; Tudor, M. J. & Beeby, S. P. (2010). Strategies for increasing the operating frequency range of vibration energy harvesters: a review. *Meas. Sci. Technol.*, Vol. 21, 022001.

Zhu, H.; Pruvost, S.; Guyomar, D. & Khodayari, A. (2009). Thermal energy harvesting from $Pb\left(Zn_{1/3}Nb_{2/3}\right)_{0.955}Ti_{0.045}O_3$ single crystals phase transitions. *J. Appl. Phys.*, Vol. 106, 124102.

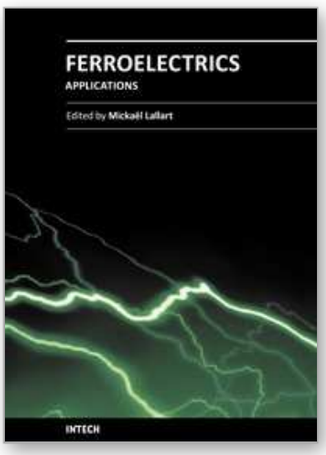

Ferroelectrics - Applications
Edited by Dr. MickaÃ«l Lallart

ISBN 978-953-307-456-6
Hard cover, 250 pages
Publisher InTech
Published online 23, August, 2011
Published in print edition August, 2011

Ferroelectric materials have been and still are widely used in many applications, that have moved from sonar towards breakthrough technologies such as memories or optical devices. This book is a part of a four volume collection (covering material aspects, physical effects, characterization and modeling, and applications) and focuses on the application of ferroelectric devices to innovative systems. In particular, the use of these materials as varying capacitors, gyroscope, acoustics sensors and actuators, microgenerators and memory devices will be exposed, providing an up-to-date review of recent scientific findings and recent advances in the field of ferroelectric devices.

InTech Europe
University Campus STeP Ri
Slavka Krautzeka 83/A
51000 Rijeka, Croatia
Phone: +385 (51) 770 447
Fax: +385 (51) 686 166
www.intechopen.com

InTech China
Unit 405, Office Block, Hotel Equatorial Shanghai
No.65, Yan An Road (West), Shanghai, 200040, China
中国上海市延安西路65号上海国际贵都大饭店办公楼405单元
Phone: +86-21-62489820
Fax: +86-21-62489821

IntechOpen